The importance of considering depth-resolved photochemistry in snow: a radiative-transfer study of NO_2 and OH production in Ny-Ålesund (Svalbard) snowpacks

J.L. FRANCE,[1] M.D. KING,[1] J. LEE-TAYLOR[2]

[1]*Department of Earth Sciences, Royal Holloway, University of London, Egham, Surrey TW20 0EX, UK*
E-mail: m.king@es.rhul.ac.uk
[2]*National Center for Atmospheric Research, PO Box 3000, Boulder, Colorado 80305, USA*

ABSTRACT. Solar visible radiation can penetrate 2–30 cm (e-folding depth) into snowpacks and photolyse nitrate anions and hydrogen peroxide contained in the snow. Photolysis rate coefficients, *J*, for NO_3^- and H_2O_2 photolysis are presented for a melting and a fresh snowpack at Ny-Ålesund, Svalbard. Calculations of (a) transfer velocities, ν, and molecular fluxes of gaseous NO_2 from the snowpack and (b) depth-integrated production rates of OH radicals within the snowpack are presented. The results show the importance of considering the depth dependence, i.e. not just the snow surface, when modelling snowpack photochemistry. Neglecting photochemistry under the snow surface can result in an apparent larger molecular flux of NO_2 from NO_3^- photolysis than the melting snowpack. However, when the depth-resolved molecular fluxes of NO_2 within the snowpack are calculated, a larger NO_2 flux may be apparent in the melting snowpack than the fresh snowpack. For solar zenith angles of 60°, 70° and 80° the modelled molecular fluxes of NO_2 from fresh snowpack are 11.6, 5.6 and 1.7 nmol m^{-2} h^{-1}, respectively, and those for melting snowpack are 19.7, 9.1 and 2.9 nmol m^{-2} h^{-1}, respectively.

INTRODUCTION

Snowpack hydroxyl radicals, OH, have been implicated in the production of gaseous fluxes from snowpack to the lower atmosphere (e.g. formaldehyde and acetaldehyde (Shepson and others, 1996; Hutterli and others, 1999; Sumner and Shepson, 1999; Couch and others, 2000; Dassau and others, 2002; Grannas and others, 2002; Houdier and others, 2002; Hutterli and others, 2003, 2004; Mabilia and others, 2007) and the fluxes of many other species such as halogens, alkenes, alkyl nitrates, peroxides and organic acids (Couch and others, 2000; Boudries and others, 2002; Dassau and others, 2002; Dibb and Arsenault, 2002; Grannas and others, 2002; Guimbaud and others, 2002; Frey and others, 2009)). Laboratory studies have demonstrated the formation of OH radicals within snowpack from the photolysis of nitrate (Honrath and others, 2000; Dubowski and others, 2001, 2002; Chu and Anastasio, 2003; Cotter and others, 2003; Anastasio and others, 2007; Jacobi and Hilker, 2007),

$$NO_3^- + h\nu \rightarrow NO_2 + O^-, \quad (1a)$$

$$O^- + H_2O \rightarrow OH^- + OH, \quad (1b)$$

where h is Planck's constant and ν is the frequency of the radiation, and from the photolysis of hydrogen peroxide (Chu and Anastasio, 2005; Jacobi and others, 2006; Anastasio and others, 2007),

$$H_2O_2 + h\nu \rightarrow 2OH. \quad (2)$$

In the presence of oxygen, formation of OH radicals within snowpack will create a radical-initiated oxidizing medium, allowing oxidation of chemicals in the snowpack. Trace organics in snowpack, suggested as palaeoclimate indicators in ice cores (Grannas and others, 2006), may be altered through photo-produced hydroxyl radical chemistry, and therefore may be unsuitable as palaeoindicators without a correction (Anderson and others, 2008).

Fluxes of gaseous NO_2 and HONO have been observed from snowpacks in Arctic and Antarctic environments (Beine and others, 1997, 1999, 2001, 2002a,b, 2003, 2006, 2008; Jones and others, 2001; Zhou and others, 2001; Honrath and others, 2002; Oncley and others, 2004; Kleffmann, 2007). Gaseous NO_2 is produced in snow through the photolysis of NO_3^- (Equation (1a); Honrath and others, 2000), in analogy to the liquid phase reaction (Mack and Bolton, 1999). An overall assessment of snowpack photochemistry is provided by Grannas and others (2007).

In the work discussed here, the 1997 Ny-Ålesund (Svalbard) field measurements by Gerland and others (1999) are used to determine snowpack optical properties, and to calculate NO_2 fluxes from these snowpacks and OH production rates within the snowpacks. Gerland and others (1999) measured the broadband transmission of photosynthetically active radiation (PAR; 400–700 nm) through snow, and the snow surface spectral albedo at different sites near the Ny-Ålesund base in May and June 1997. The two snowpacks described by Gerland and others (1999) are hereafter described as 'fresh' and 'melting'. Further details of these snowpacks are given in Table 1 and by Gerland and others (1999). We present calculations, with appropriate assumptions, of photolysis rate coefficients of nitrate and hydrogen peroxide photolysis within the snowpack, using the discrete-ordinate radiative transfer code (DISORT) model, TUV-snow (Lee-Taylor and Madronich, 2002). A photolytic rate coefficient, *J*, for Equations (1a) and (2), respectively, is defined by the kinetic rate equations

$$\frac{d[NO_3^-]}{dt} = -J_{(1a)}[NO_3^-] \quad (3)$$

and

$$\frac{d[H_2O_2]}{dt} = -J_{(2)}[H_2O_2], \quad (4)$$

where t is time. Photolytic rate coefficients may be calculated

https://doi.org/10.3189/002214310793146250 Published online by Cambridge University Press

Table 1. Physical, optical and chemical properties of the two snowpacks (fresh and melting) used in this work (Gerland and others, 1999) to calculate (a) absorption and scattering cross sections, (b) photolysis rate coefficients and (c) hydroxyl radical production rates for both melting and fresh snowpacks at Ny-Ålesund in 1997

Snow type*	e-fold†	Albedo*	$H_2O_{(l)}$‡	Measurement date*	Daily column ozone§	Average column ozone§	Snow density*	Snow temp.*	$[NO_3^-]$¶	$[H_2O_2]$‖	σ^+_{abs}**	σ_{scatt}**
	cm		%		DU	DU	g cm^{-3}	°C	nmol cm^{-3}	nmol cm^{-3}	cm^2 kg^{-1}	m^2 kg^{-1}
Fresh	6	0.97	2	19 May 1997	325	310	0.45	–2	1	4	2.7	16.7
Melting	9.9	0.69	9	19 Jun 1997	375	310	0.45	0	1	4	19.8	0.8

*Data from (or determined from) Gerland and others (1999).
†Data derived from PAR measurements in snow (Gerland and others, 1999).
‡Water equivalent content of snow at 10 cm depth in the snowpack, from Gerland and others (1999).
§Ozone data from the NASA TOMS programme.
¶Typical concentrations of NO_3^- in Arctic snow; values are per cm^3 of snow.
‖Typical concentrations of H_2O_2 in snow; values are per cm^3 of snow.
**Derived values at a wavelength of 400 nm (this work).

by integrating the product of the chromophore (i.e. nitrate or hydrogen peroxide) absorption cross section, $\sigma(\lambda,T)$, the chromophore quantum yield, $\Phi(\lambda,T)$, and the spherical irradiance, $F(\lambda)$, over the wavelength of the irradiance, λ, at a known temperature:

$$J = \int_{\lambda_1}^{\lambda_2} \sigma(\lambda, T)\, \Phi(\lambda, T)\, F(\lambda)\, \mathrm{d}\lambda. \quad (5)$$

The reported values of light attenuation and albedo (Gerland and others, 1999) are used to optically characterize the snowpack for the TUV-snow model using a previously described method (e.g. Fisher and others, 2005). The depth-resolved photolysis rate coefficients of nitrate and hydrogen peroxide are then used to calculate the formation rate of OH radicals within the snowpack, and the fluxes of NO_2 from the snowpack. The photolytic rate coefficients of Equations (1) and (2) depend upon the optical properties of the snowpack, described by a scattering and an absorption coefficient. Values for these coefficients may be constrained by observations of albedo, e-folding depth (characteristic distance over which the diffuse irradiance in the snowpack decays to 1/e or ~37% of its initial value (King and Simpson, 2001)) and snow density. Measurements of albedo, light transmission and density were recorded by Gerland and others (1999) for fresh and melting snowpacks. The validity of using the TUV-snow DISORT radiative-transfer coding (Lee-Taylor and Madronich, 2002) to describe photochemistry in snow was borne out in experiments by Phillips and Simpson (2005) that showed good agreement between photolysis of a chromophore within laboratory snow and predictions based on the TUV-snow model.

METHODS

The TUV-snow model (Lee-Taylor and Madronich, 2002) employs an eight-stream pseudo-spherical, discrete-ordinates, radiative-transfer scheme (Stamnes and others, 1988). It allows optical characterization of a snowpack from knowledge of albedo and light transmission into the snowpack, without the need for knowledge of snow grain size. The optical information is used to derive a wavelength-dependent absorption coefficient for absorption by impurities within the snowpack, σ^+_{abs}, and a wavelength-independent scattering coefficient, σ_{scatt}. A detailed description of the modelling process to find values for these coefficients is given by Lee-Taylor and Madronich (2002).

The parameters used to derive the absorption cross section, σ^+_{abs}, and scattering cross section, σ_{scatt}, for the two snowpacks assumes an under-snow ground albedo of 0.1, no atmospheric aerosol, and stratospheric ozone columns of 325 and 375 DU (Dobson units; daily values for 19 June 1997 (melting snow) and 19 May 1997 (fresh snow), respectively). Ozone column data were taken from the NASA Total Ozone Massing Spectrometer (TOMS) programme (McPeters and others, 1998). Earth–sun distances were calculated for the dates of the original snowpack measurements and are needed to calculate solar irradiance at the top of the atmosphere. The absorption cross section of ice was taken from Warren and Brandt (2008). Values of e-folding depths are kept constant over the wavelength range 400–700 nm, as only PAR (cumulative radiation over wavelengths from 400 to 700 nm) attenuation is reported by Gerland and others (1999). Spectral albedo data between 350 and 1300 nm are reported by Gerland and others (1999). Values are derived for σ^+_{abs} and σ_{scatt} cross sections for the two types of snowpack at 400 nm, and the values derived for σ^+_{abs} and σ_{scatt} at 400 nm are used to calculate photolysis rate coefficients for Equations (1a) and (2). King and Simpson (2001) show that e-folding depth varies by only ~9% over the wavelength range 330–400 nm, suggesting that it is reasonable to use values of σ^+_{abs} and σ_{scatt} assessed at 400 nm. The aqueous ultraviolet (UV) absorption cross section of hydrogen peroxide and nitrate anion decreases rapidly with increasing wavelength in the 320 nm region. The irradiance of incident solar radiation increases rapidly with increasing wavelength in this region. The product of these two functions results in a new function that peaks around 320 nm as shown by Chu and Anastasio (2005, 2008). Using values of σ^+_{abs} and σ_{scatt} at 400 nm to calculate photolysis rate coefficients of nitrate and hydrogen peroxide is also consistent with previous work (King and Simpson, 2001; Lee-Taylor and Madronich, 2002; Fisher and others, 2005; Beine and others, 2006; France and others, 2007).

The TUV-snow model can predict photolysis rate coefficients at any number of depths within snowpacks with a minimum resolution of 1 mm, provided that σ^+_{abs}, σ_{scatt}, the snowpack density, ρ, location, time, ozone column depth and sky conditions are known (Lee-Taylor and Madronich,

https://doi.org/10.3189/002214310793146250 Published online by Cambridge University Press

2002). In this work, 30 unequally spaced separate snowpack layers, with more thin layers near the snow surface, within a 1 m deep and laterally semi-infinite snowpack slab were used. The layer spacing is the same as used by Lee-Taylor and Madronich (2002). Photolysis rate constants, J, are calculated for each snow layer for Equations (1) and (2). Depth-integrated photolysis rate coefficients (also known as transfer velocities), υ, for the production of NO_2 (υ_{NO_2}) and OH (υ_{OH}) radical from the photolysis of NO_3^- and H_2O_2 in snow, respectively, are calculated as

$$\upsilon_{NO_2} = \int_{z=0}^{z=1} J_{(1a)}\,dz, \quad (6)$$

$$\upsilon_{OH} = 2\int_{z=0}^{z=1} J_{(2)}\,dz, \quad (7)$$

where $J_{(1a)}$ and $J_{(2)}$ are the photolysis rate coefficients for Equations (1a) and (2), respectively, and z is the snowpack depth with $z = 1$ m the snowpack surface and $z = 0$ m the snowpack interface with the ground.

Gerland and others (1999) reported snow thicknesses for some of their melting-snow pits of 0.48 and 0.78 m where PAR transmission through the snowpack was measured. For modelling in this work, we use a 1 m thick snowpack to ensure an optically semi-infinite snowpack (Lee-Taylor and Madronich, 2002). The minimum snowpack depth to ensure an optically semi-infinite snowpack was discussed by Gerland and others (1999) and suggested from a review of literature to be 50 cm for the snowpacks studied in this work. The issue of minimum depth for semi-infinite snowpack has also been investigated by France (2008) who found the molecular flux (and depth-integrated production rate) from Equation (2) was independent of snowpack depth provided the snowpack is thicker than three e-folding depths, i.e. ~0.3 m for the melting snowpack (and 0.18 m for the fresh snowpack). Thus, whether the snowpack thickness is 0.3, 0.48. 0.78 or 1 m makes a negligible (<3%) difference to the flux of material from the snowpack. The irradiance of light in the snowpack decays exponentially with depth below the first few cm. For melting-snowpack thicknesses less than 0.3 m, the albedo of the ground underlying the snowpack will become significant in determining snow surface albedo. Melting snowpacks less than 0.3 m thick are not considered here, as the main aim is to show the importance of considering photochemistry at depth within the snowpack.

For calculating photolysis rate coefficients (Equation (5)), the absorption cross section for hydrogen peroxide was taken from Chu and Anastasio (2005), and the nitrate absorption cross section from Burley and Johnston (1992), for consistency with our previous studies (Simpson and other 2002; Fisher and others 2005; France and others 2007; Beine and others 2008). The temperature-dependent quantum yields used to calculate nitrate and hydrogen peroxide photolysis rate coefficients are taken from Chu and Anastasio (2003, 2005, respectively). The snowpack modelling in this study uses snowpack temperatures from Gerland and others (1999) (Table 1).

The predicted molecular flux of NO_2, $F_{NO_3^-}(NO_2)$, from the snowpack to the atmosphere, owing to nitrate photolysis within the snowpacks, is

$$F_{NO_3^-}(NO_2) = [NO_3^-]\,\upsilon_{NO_2} = [NO_3^-]\int_{z=0}^{z=1} J_{(1)}\,dz, \quad (8)$$

assuming that all the NO_2 formed from the photolytic reaction (Equation (1)) can escape the snowpack. Depth-integrated production rates of OH radicals are calculated for Equations (2) and (1), respectively:

$$F_{H_2O_2}(OH) = [H_2O_2]\,\upsilon_{OH} = [H_2O_2]\int_{z=0}^{z=1} J_{(2)}\,dz, \quad (9)$$

$$F_{NO_3^-}(OH) = [NO_3^-]\,\upsilon_{NO_2} = [NO_3^-]\int_{z=0}^{z=1} J_{(1)}\,dz. \quad (10)$$

It is assumed that in-snow concentrations of NO_3^- and H_2O_2 are independent of depth, and that Equation (1a) is the rate-limiting step in producing OH radicals from nitrate photolysis. Equations (8) and (10) are mathematically the same: Equation (1) produces one NO_2 molecule and one OH radical, but for clarity we have written out the equation for each chemical reaction. Note we term $F_{NO_3^-}(NO_2)$ a molecular flux of NO_2 from the snowpack, whereas we term $F_{H_2O_2}(OH)$ a depth-integrated production rate because the OH radicals are too reactive to leave the snowpack. The terms 'flux' and 'depth-integrated production rate' continue the nomenclature used for similar work (e.g. France and others, 2007).

Nitrate concentrations in Svalbard snowpacks are taken from five studies and adjusted to a nitrate concentration per unit volume of snow (as opposed to liquid water). Beine and others (2003) reported nitrate concentrations of 0.47–3.8 nmol cm^{-3}, with a typical value of 1.26 nmol cm^{-3}. They noted that anion concentration in the snowpack was very varied horizontally and vertically, owing to wind events. Heaton and others (2004) reported nitrate values in snow of 0.9–1.8 nmol cm^{-3} (fresh) and 0.45–3.6 nmol cm^{-3} (older). Semb and others (1984) found nitrate concentrations in surface snow of <0.45–1.8 nmol cm^{-3} and reasonably invariant concentration depth profiles. By crude visual interpolation of the values reported by Grannas and others (2007), one can deduce nitrate anion concentrations in snow of 0.87–1.09 nmol cm^{-3}. The nitrate data from the Arctic Monitoring and Assessment Program report (AMAP, 1998) could not be used in this study. Nitrate concentrations in snow for other archipelagos in the Arctic Ocean are ~0.9 nmol cm^{-3} for Franz Josef Land (Nickus, 2003) and 0.36–1.09 nmol cm^{-3} for Severnaya Zemlya (Opel and others, 2009). Nickus (2003) and Opel and others (2009) noted that nitrate concentrations correspond well to the values found in Greenland, parts of the Canadian Arctic and Alaska and that concentration–depth profiles in Severnaya Zemlya are similar to those from Svalbard. For the studies reported here, a nitrate in snow concentration of 1 nmol cm^{-3} is used based on the above measurements.

The authors are unaware of any snow hydrogen peroxide concentration measurements for Svalbard, so the work presented here has had to rely on data presented for Summit, Greenland, and South Pole. Studies of hydrogen peroxide concentration in south polar snow report values of 1.35–6.75 nmol cm^{-3} (Hutterli and others, 2004), 0.9–9.9 nmol cm^{-3} (McConnell and others 1997) and 0.9–9 nmol cm^{-3} (McConnell and others 1998). For Summit, concentrations are typically 0.27–7.92 nmol cm^{-3} (Hutterli and others, 2003), with annual means of 1.56–3.52 nmol cm^{-3} (Anklin and Bales, 1997) and ~2–16 nmol cm^{-3} variation in depth and surface snow (Anastasio and others 2007). Hydrogen peroxide values between sites are similar, in part reflecting the local source

https://doi.org/10.3189/002214310793146250 Published online by Cambridge University Press

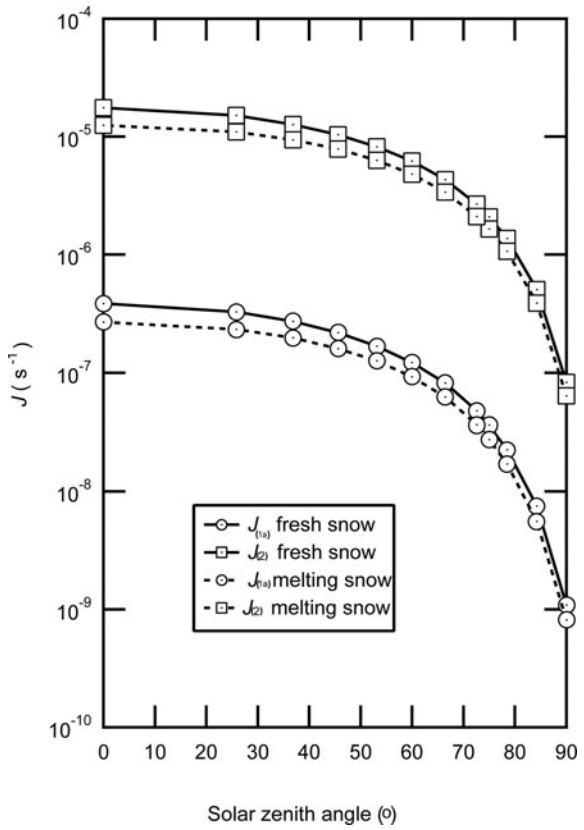

Fig. 1. Photolysis rate coefficients for NO_3^- and H_2O_2 at the snow surface, $J_{(1a)}$ and $J_{(2)}$, versus solar zenith angles 0–90° for both melting and fresh snowpack. $J_{(1a)}$ is the coefficient for photolysis of nitrate, and $J_{(2)}$ is the coefficient for photolysis of hydrogen peroxide. Values of $J_{(1a)}$ and $J_{(2)}$ are larger for fresh snow.

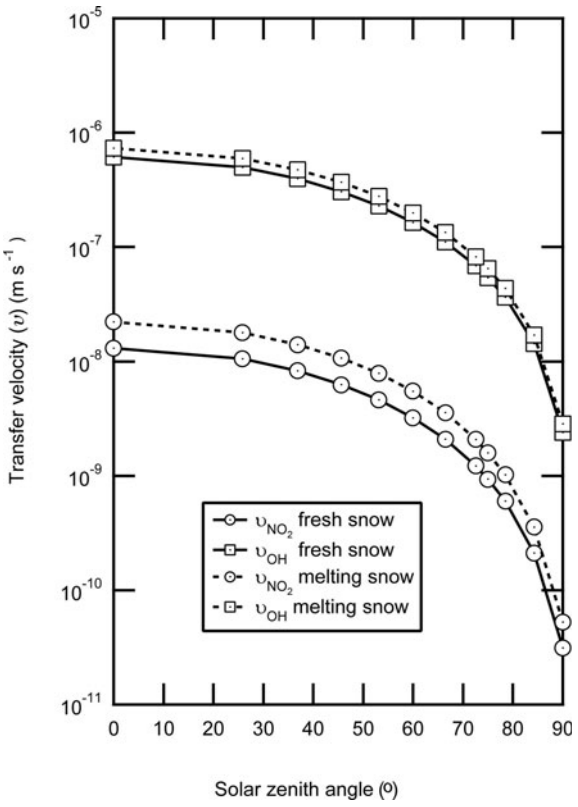

Fig. 2. Depth-integrated photolysis rate coefficients (i.e. transfer velocities), $\upsilon_{NO_3^-}$ and $\upsilon_{H_2O_2}$, for a 1 m deep snowpack versus 0–90° solar zenith angles, for both melting and fresh snowpacks. Values of $\upsilon_{NO_3^-}$ and $\upsilon_{H_2O_2}$ are larger for melting snow, in contrast to Figure 1.

of H_2O_2 from deposition following gas-phase generation in the atmosphere, whereas nitrate is associated with precipitation and deposition. Surface snow concentrations of H_2O_2 in snow vary seasonally, with large values in spring and small values in winter. Seasonal variation of the concentration of H_2O_2 in surface snow results in a depth dependence of H_2O_2 concentrations. Here a value of 4 nmol cm^{-3} in snow (invariant with depth) is considered, and later in the discussion the small effect of a concentration–depth dependence on molecular fluxes out of the snowpack.

The molecular fluxes (or depth-integrated production rates), calculated by Equations (8–10), are linearly proportional to the snowpack concentration of nitrate and hydrogen peroxide. Thus, the reader can adjust the molecular fluxes reported in this paper for their values of the concentration of nitrate or hydrogen peroxide in the snowpack by simply dividing the molecular flux (or depth-integrated production rate) by the concentration of nitrate or hydrogen peroxide used here and multiplying by preferred values of concentration of nitrate or hydrogen peroxide in their snowpack.

Surface photolysis rate coefficients, J, transfer velocities (depth-integrated photolysis rate coefficients), υ, and molecular fluxes (depth-integrated production rates), F, were calculated for both NO_3^- and H_2O_2 photolysis for fresh and melting snowpacks.

RESULTS

The values of scattering and absorption coefficients (Table 1) are within the range of other studies (e.g. σ^+_{abs} = 0–8 (Lee-Taylor and Madronich, 2002), 4.3–37 (Beine and others, 2006) and 0.7–1 (Fisher and others, 2005); and σ_{scatt}=1.1–30 (Lee-Taylor and Madronich, 2002), 1–6 (Beine and others, 2006) and 1–5 (Fisher and others, 2005)). The fresh Ny-Ålesund snowpack is optically most similar to Arctic spring wind-blown snowpack (King and Simpson, 2001), and the melting Ny-Ålesund snowpack is optically transitional between coastal maritime Antarctic wind-blown (Beine and others, 2006) and Arctic summer melting snowpack (Grenfell and Maykut, 1977).

Figures 1 and 2 show surface and depth-integrated photolysis rate coefficients, J, and transfer velocities, υ, for Equations (1a) and (2) versus solar zenith angles 0–90° for both snowpack types at Ny-Ålesund based on the assumptions discussed. In Figure 1, the surface photolysis rate coefficients are larger for the fresh snow than for the melting snow, but in Figure 2 the transfer velocities are larger for the melting snow than for the fresh snow. Using the surface photolysis rate coefficients (Fig. 1) instead of the depth-integrated photolysis rate coefficients (Fig. 2) can lead to errors in calculation of the fluxes of NO_2 from the snowpack. Considering only the surface photolysis rate coefficients to calculate NO_2 fluxes will lead to the false conclusion that the fresh Ny-Ålesund snowfall will produce a larger flux than the melting snowpack. The authors consider this issue a result that demonstrates the importance of modelling photolysis rate coefficients for a whole snowpack rather than considering just the surface snow layer. A similar argument can be constructed for the depth-integrated production rates of OH radicals.

https://doi.org/10.3189/002214310793146250 Published online by Cambridge University Press

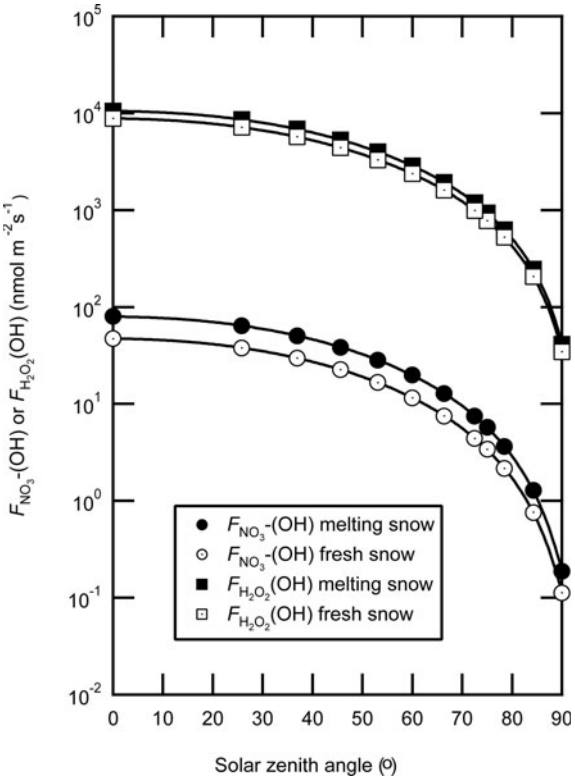

Fig. 3. Depth-integrated production rates, $F_{NO_3^-}(OH)$ and $F_{H_2O_2}(OH)$, at 0–90° solar zenith angles for both melting and fresh snowpacks.

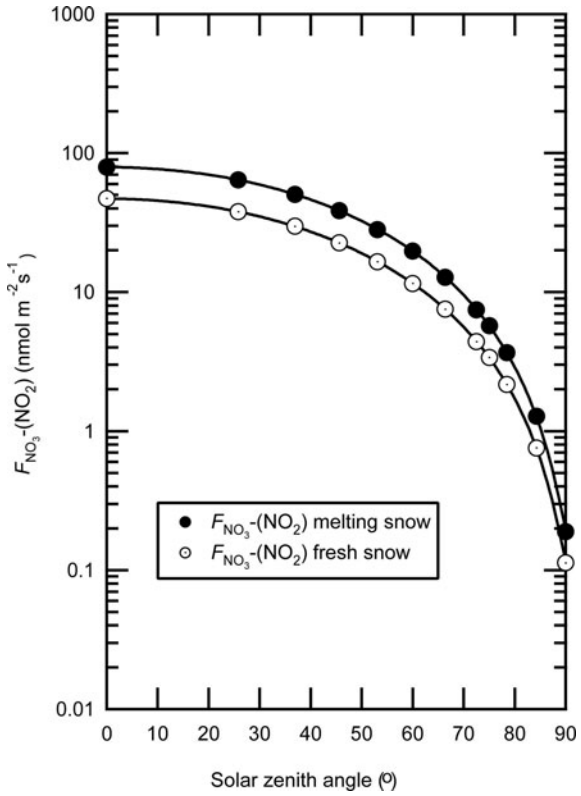

Fig. 4. Flux of NO_2 produced in 1 m of fresh and melting snowpack from the photolysis rate of NO_3^- for 30–90° solar zenith angles with clear sky conditions.

Depth-integrated production rates of OH radicals from the photolysis of NO_3^- and H_2O_2 are shown in Figure 3. Hydroxy radical production from H_2O_2 photolysis is over 100 times larger than from NO_3^- photolysis, as has been shown by Chu and Anastasio (2005) for surface OH production and by France and others (2007) for depth-integrated OH production rates at other snowpack sites. The results plotted in Figure 3 show that depth-integrated OH production rates are larger within the melting snowpack than within the fresh snowpack.

The molecular fluxes of gaseous NO_2 from melting and fresh snowpack at Ny-Ålesund for solar zenith angles of 30–90° and clear sky conditions are shown in Figure 4. For solar zenith angles of 60°, 70° and 80° the modelled fluxes of NO_2 from the fresh snowpack are 11.6, 5.6 and 1.7 nmol $m^{-2}\,h^{-1}$, respectively, while for the melting snowpack they are 19.7, 9.1 and 2.9 nmol $m^{-2}\,h^{-1}$, respectively.

DISCUSSION

For the two snowpacks considered here, the predicted fluxes of NO_2 from the snowpack to the atmosphere are comparable with values of NO_x observed in other snowpack studies (Table 2). Maximum fluxes of NO_x above the snowpack have been measured to be ~40 nmol $m^{-2}\,h^{-1}$ at Alert, Canada (Beine and others, 2002a,b), 30 nmol $m^{-2}\,h^{-1}$ at South Pole (Oncley and others, 2004) and 13 nmol $m^{-2}\,h^{-1}$ at Neumayer, Antarctica (Wolff and others, 2002). The maximum solar zenith angle was 68° for the South Pole campaign and approximately 60° for the Neuymayer and Alert studies.

The modelled fluxes of NO_2 leaving the snowpack using the TUV-snow model for the fresh and melting Ny-Ålesund snowpacks at a solar zenith angle of 60° are 11.6 and 19.7 nmol $m^{-2}\,h^{-1}$ respectively. Thus, the magnitude of modelled NO_x fluxes above Ny-Ålesund snowpack is consistent with previous measurements at other sites. The actual molecular flux of NO_2 from the snowpack may be affected by secondary processes, such as photolysis of NO_2 before venting from the snowpack or snow microphysics preventing the release of NO_2 from the snowpack. Boxe and others (2003, 2005, 2006) showed that emission rates of gaseous NO_2 from irradiated ice (containing nitrate anions) increase with increasing ice temperature. Gaseous emissions of NO_2 are partially controlled by mass transfer, and hence the morphology, of polycrystalline ice (Boxe and others, 2006). Laboratory experiments by Boxe and others (2003, 2005) showed that photolysis of nitrate in polycrystalline ice produces large NO_2 emissions above an ice temperature of –8°C. Boxe and others (2006) could not reproduce the $[NO_2]/[NO]$ ratio in field measurement studies, but Boxe and others (2003, 2005, 2006) did demonstrate that there may be some loss of photogenerated NO_2 in snowpack. NO_2 loss in snowpack is minimal at higher ice temperatures. Both snowpacks considered here have temperatures greater than –8°C, and the comparative nature of this work means the loss of photogenerated NO_2 is not critical for the main result. The availability in the Arctic environment of NO_x from snowpack emissions has been shown to have a substantial impact upon the oxidative capacity of the lower troposphere, especially in the spring (Morin and others, 2008).

Previous work has shown that UV radiation penetrates deeper into warmer, wetter snows with larger grain sizes than into colder, drier, smaller-grained snowpacks, so wetter snowpacks have larger photolysis rate coefficients at depth

https://doi.org/10.3189/002214310793146250 Published online by Cambridge University Press

Table 2. Comparison of modelled NO_2 fluxes from melting and fresh Ny-Ålesund snowpack with NO_x measurements from previous snowpack studies. SZA: solar zenith angle

	Ny-Ålesund, Svalbard (modelled, SZA 60°)		Neumayer, Antarctic (Jones and others, 2000)	Summit, Greenland (Honrath and others, 2002)	South Pole (Oncley and others, 2004)	Alert, Canada (Beine and others, 2002a,b)
	Melting	Fresh				
$F_{NO_3^-}(NO_2)$(nmol m^{-2} h^{-}1)	19.7	11.6	13	36	30	30
$[NO_3^-]$ (nmol cm^{-3})	1	1	0.65*	4†	6.7‡	8§
Maximum SZA during campaign (°)			56	49	68	66

*Wolff and others (2002). †Dibb and others (1998). ‡Dibb and others (2004); Hutterli and others (2004). §Simpson and others (2002).

(Fisher and others, 2005). The melting snowpack described by Gerland and others (1999) and modelled in this work may be considered as a maritime snowpack using the classification from Sturm and others (1995) and is similar to the Scottish snowpack described by Fisher and others (2005). The melting snowpack has a higher measured liquid water content than the fresh snowpack (Gerland and others, 1999), and as expected has a lower value of σ_{scatt} than the fresh snowpack, as liquid water effectively increases snow grain size (Warren, 1982). The measured electrical conductivities of the fresh and melting snowpacks from Ny-Ålesund are similar within the top 10 cm of snowpack (Gerland and others, 1999). Photochemistry occurs mainly in the top 10 cm of the the snowpack, so it is speculated that ionic chemical concentrations in the two snowpacks are similar, supporting the assumption that the concentrations of nitrate and hydrogen peroxide have similar values in each snowpack. The assumption that the concentrations of nitrogen and hydrogen peroxide have similar values in each snowpack is not critical here, as our aim is to demonstrate the effect of considering photolysis at depth in the snowpack. The large difference in absorption between the two snowpacks is probably due to depositional accumulation of coloured, non-ionic chemicals (e.g. black carbon or humic material) as the snowpack ages. The older, melting snowpack, having had longer to accumulate such absorbers, will thus have a higher value of σ^+_{abs}. The presence of absorbers in snowpack has been shown to cause a climatic feedback loop, leading to further melting of the snowpack due to lowering of the surface albedo, and thus increasing the absorption of solar radiation (Qian and others, 2009). The TUV-snow model uses a monochromatic black carbon absorber to determine the absorption coefficient, which is a good first approximation to Svalbard soil with its high coal content (France, 2008).

An interesting result of this work is the comparison between surface photolysis rate coefficients and depth-integrated photolysis rate coefficients. The origin of the larger depth-integrated photolysis rate coefficients in the melting snow, and of the larger surface photolysis rate coefficients in the fresh snow, is shown in Figure 5. The large value of albedo and the shorter e-folding depth in the fresh snow give larger values of surface photolysis rate coefficients, but little penetration into the snowpack compared to the melting snowpack. The photolysis rate coefficient–depth profiles for the two snowpacks are equal at approximately 2 cm (nitrate) and 5 cm (hydrogen peroxide) depth in the snowpack. The value of the fresh-snowpack photolysis rate coefficient decreases faster with depth than the melting-snowpack photolytic rate constant. Integration of the photolysis rate coefficient over the depth for the snowpacks results in a larger flux of the melting snowpack than of the fresh snowpack. Therefore, snowpack photolytic emission fluxes should always be calculated using depth-integrated photolysis rate coefficients, not just surface photolysis rate coefficients.

Nitrate and hydrogen peroxide concentrations vary with season and depth within the snowpack. Here the concentration–depth profile of nitrate and hydrogen peroxide is considered constant. France and others (2007) undertook a sensitivity study of the effect of three different concentration–depth profiles on the calculated molecular fluxes (and depth-integrated production rates) using the same model used here. They showed that for hydrogen peroxide photolysis the differences in calculated depth-integrated production rates of hydroxyl radical were negligible when comparing (1) a concentration–depth profile of hydrogen peroxide from a field study, (2) a constant surface concentration of hydrogen peroxide, invariant with depth, and (3) a constant concentration of hydrogen peroxide averaged over the equivalent of two e-folding depths, but invariant with depth. They repeated the calculation for nitrate photolysis using three comparable concentration–depth profiles and noted that agreement between the three calculations was within a factor of two, i.e. a much smaller uncertainty than the natural variation in concentrations of nitrate in surface snow at Ny-Ålesund, as reported by Beine and others (2003). The depth dependence of the nitrate or hydrogen peroxide has little effect on the flux (or depth-integrated production rate) because the concentration of hydrogen peroxide or nitrate may only decrease by a factor of four over the depth of a snow pit, whereas the spherical solar irradiance will decrease exponentially with depth (a few cm below the surface).

To test the sensitivity of depth-integrated production rates to the initial values of albedo and e-folding depth, the depth-integrated production rate of OH radicals in the melting snowpack was recalculated using 90% of the original albedo and 110% of the original e-folding values to generate a lower limit of σ^+_{abs} and σ_{scatt}, and 110% of the original albedo and 90% of the original e-folding values to generate upper values of σ^+_{abs} and σ_{scatt}. These newly derived values were used to calculate upper- and lower-limit depth-integrated rates for OH radical production from NO_3^- and H_2O_2 photolysis. The resulting uncertainty is insensitive to solar zenith angle, and

https://doi.org/10.3189/002214310793146250 Published online by Cambridge University Press

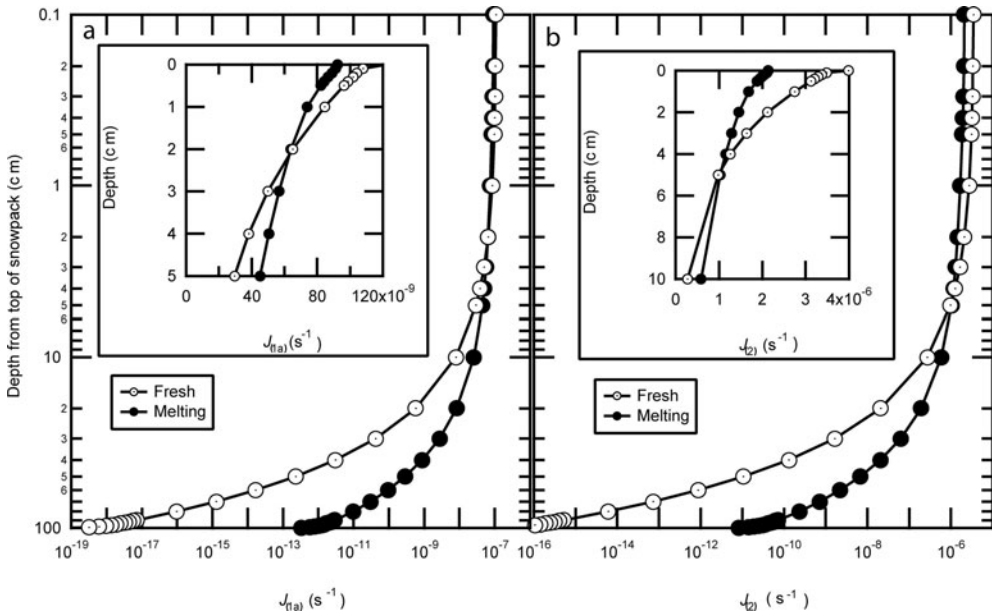

Fig. 5. Photolysis rate coefficients versus depth within a 1 m deep snowpack for both melting and fresh Ny-Ålesund snow: (a) for photolysis of nitrate, and (b) for photolysis of hydrogen peroxide. The inserts are the same data at larger scale for the region where the photolysis rate constants of fresh and melting snowpack are equal.

equal to $\pm^{8\%}_{11\%}$. Thus, fortuitously, a 10% error on both albedo and e-folding depth results in approximately a 10% error in depth-integrated production rates (fluxes).

CONCLUSIONS

Calculated depth-resolved photolysis rate coefficients of NO_3^- anions and H_2O_2, along with depth-integrated OH production rates and molecular fluxes of NO_2, for melting and fresh snowpacks at Ny-Ålesund show the importance of using a depth-resolved method to model photolysis rate coefficients in snowpack, rather than considering only the surface photolysis rate coefficients. The depth-integrated photolysis rate coefficients are greater for melting snow than for fresh snow. This study shows the importance of always considering the photochemistry of the total snowpack, not just of the snow surface.

Modelled fluxes from the two snowpacks, of NO_2 due to NO_3^- photolysis, at appropriate solar zenith angles are of the same order of magnitude as NO_x fluxes measured at other snowpack sites. Hydroxyl radical production from both snowpacks is dominated by H_2O_2 photolysis.

ACKNOWLEDGEMENTS

J.L.F. thanks the UK Natural Environment Research Council (NERC) for financial support through studentship NER/S/A/200412177. M.D.K. thanks the Programma Nazionale di Ricerche in Antartide (PNRA) for support through project 2004/6.2, the Royal Society for grant 54006.G503/24054/SM and the NERC Field Spectroscopy Facility (FSF) for grant 489.1205, and the Research Committee of the Geology Department of Royal Holloway, University of London. J.L.F. and M.D.K. acknowledge assistance from NERC grants NE/F010788/1 and NE/F004796/1. The National Center for Atmospheric Research is sponsored by the US National Science Foundation.

REFERENCES

Anastasio, C., E.S. Galbavy, M.A. Hutterli, J.F. Burkhart and D.K. Friel. 2007. Photoformation of hydroxyl radical on snow grains at Summit, Greenland. *Atmos. Environ.,* **41**(24), 5110–5121.

Anderson, C.H., J.E. Dibb, R.J. Griffin, G.S.W. Hagler and M.H. Bergin. 2008. Atmospheric water-soluble organic carbon measurements at Summit, Greenland. *Atmos. Environ.,* **42**(22), 5612–5621.

Anklin, M. and R.C. Bales. 1997. Recent increase in H_2O_2 concentration at Summit Greenland. *J. Geophys. Res.*, **102**(D15), 19,099–19,104.

Arctic Monitoring and Assessment Program (AMAP). 1998. *AMAP assessment report: Arctic pollution issues*. Oslo, Arctic Monitoring and Assessment Program.

Beine, H.J. *and 6 others*. 1997. NO_x during ozone depletion events in the arctic troposphere at Ny-Ålesund, Svalbard. *Tellus B,* **49**(5), 556–565.

Beine, H.J., A. Dahlback and J.B. Ørbaek. 1999. Measurements of $J(NO_2)$ at Ny-Ålesund, Svalbard. *J. Geophys. Res.,* **104**(D13), 16,009–16,019.

Beine, H.J., I. Allegrini, R. Sparapani, A. Ianniello and F. Valentini. 2001. Three years of springtime trace gas and particle measurements at Ny-Ålesund, Svalbard. *Atmos. Environ.,* **35**(21), 3645–3658.

Beine, H.J., R.E. Honrath, F. Dominé, W.R. Simpson and J.D. Fuentes. 2002a. NO_x during background and ozone depletion periods at Alert: fluxes above the snow surface. *J. Geophys. Res.,* **107**(D21), 4584. (10.1029/2002JD002082.)

Beine, H.J. *and 6 others*. 2002b. Snow-pile and chamber experiments during the Polar Sunrise Experiment 'Alert 2000': exploration of nitrogen chemistry. *Atmos. Environ.,* **36**(15–16), 2707–2719.

Beine, H.J. *and 6 others*. 2003. Fluxes of nitrates between snow surfaces and the atmosphere in the European high arctic. *Atmos. Chem. Phys.,* **3**(1), 335–346.

Beine, H.J. *and 6 others*. 2006. Surprisingly small HONO emissions from snow surfaces at Browning Pass, Antarctica. *Atmos. Chem. Phys.,* **6**(9), 2569–2580.

Beine, H., A.J. Colussi, A. Amoroso, G. Esposito, M. Montagnoli and M.R. Hoffmann. 2008. HONO emissions from snow

https://doi.org/10.3189/002214310793146250 Published online by Cambridge University Press

surfaces. *Environ. Res. Lett.,* **3**(4), 045005. (10.1088/1748-9326/3/4/045005.)

Boudries, H. *and 7 others*. 2002. Distribution and trends of oxygenated hydrocarbons in the high Arctic derived from measurements in the atmospheric boundary layer and interstitial snow air during the ALERT2000 field campaign. *Atmos. Environ.,* **36**(15–16), 2573–2583.

Boxe, C.S. *and 8 others*. 2003. Multiscale ice fluidity in NO_x photodesorption from frozen nitrate solutions. *J. Phys. Chem. A,* **107**(51), 11,409–11,413.

Boxe, C.S. *and 6 others*. 2005. Photochemical production and release of gaseous NO_2 from nitrate-doped water ice. *J. Phys. Chem. A,* **109**(38), 8520–8525.

Boxe, C.S., A.J. Colussi, M.R. Hoffmann, I.M. Perez, J.G. Murphy and R.C. Cohen. 2006. Kinetics of NO and NO_2 evolution from illuminated frozen nitrate solutions. *J. Phys. Chem. A,* **110**(10), 3578–3583.

Burley, J.D. and H.S. Johnston. 1992. Ionic mechanisms for heterogeneous stratospheric reactions and ultraviolet photoabsorption cross sections for NO_2^+, HNO_3, and NO_3^- in sulfuric acid. *Geophys. Res. Lett.*, **19**(13), 1359–1362.

Chu, L. and C. Anastasio. 2003. Quantum yields of hydroxyl radical and nitrogen dioxide from the photolysis of nitrate on ice. *J. Phys. Chem. A,* **107**(45), 9594–9602.

Chu, L. and C. Anastasio. 2005. Formation of hydroxyl radical from the photolysis of frozen hydrogen peroxide. *J. Phys. Chem. A,* **109**(28), 6264–6271.

Chu, L. and C. Anastasio. 2008. Formation of hydroxyl radical from the photolysis of frozen hydrogen peroxide (correction). *J. Phys. Chem. A,* **112**(12), 2747–2748.

Cotter, E.S.N., A.E. Jones, E.W. Wolff and S.B. Baugitte. 2003. What controls photochemical NO and NO_2 production from Antarctic snow? Laboratory investigation assessing the wavelength and temperature dependence. *J. Geophys. Res.,* **108**(D4), 4147. (10.1029/2002JD002602.)

Couch, T.L., A.L. Sumner, T.M. Dassau, P.B. Shepson and R.E. Honrath. 2000. An investigation of the interaction of carbonyl compounds with the snowpack. *Geophys. Res. Lett.,* **27**(15), 2241–2244.

Dassau, T.M. *and 10 others*. 2002. Investigation of the role of the snowpack on atmospheric formaldehyde chemistry at Summit, Greenland. *J. Geophys. Res.,* **107**(D19), 4394. (10.1029/2002JD002182.)

Dibb, J.E. and M. Arsenault. 2002. Shouldn't snowpacks be sources of monocarboxylic acids? *Atmos. Environ.,* **36**(15–16), 2513–2522.

Dibb, J.E., R.W. Talbot, J.W. Munger, D.J. Jacob and S.M. Fan. 1998. Air–snow exchange of HNO_3 and NO_y at Summit, Greenland. *J. Geophys. Res.*, **103**(D3), 3475–3486.

Dibb, J.E., L.G. Huey, D.L. Slusher and D.J. Tanner. 2004. Soluble reactive nitrogen oxides at South Pole during ISCAT 2000. *Atmos. Environ.,* **38**(32), 5399–5409.

Dubowski, V., A.J. Colussi and M.R. Hoffmann. 2001. Nitrogen dioxide release in the 302 nm band photolysis and spray-frozen aqueous nitrate solutions: atmospheric implications. *J. Phys. Chem. A,* **105**(20), 4928–4932.

Dubowski, V., A.J. Colussi, C. Boxe and M.R. Hoffmann. 2002. Monotonic increase of nitrite yields in the photolysis of nitrate in ice and water between 238 and 294 K. *J. Phys. Chem. A,* **106**(30), 6967–6971.

Fisher, F.N., M.D. King and J. Lee-Taylor. 2005. Extinction of UV-visible radiation in wet midlatitude (maritime) snow: implications for increased NO_x emission. *J. Geophys. Res.,* **110**(D21), D21301. (10.1029/2005JD005963.)

France, J.L. 2008. Chemical oxidation in snowpack. (PhD thesis, Royal Holloway, University of London.)

France, J.L., M.D. King and J. Lee-Taylor. 2007. Hydroxyl (OH) radical production rates in snowpacks from photolysis of hydrogen peroxide (H_2O_2) and nitrate (NO_3^-). *Atmos. Environ.,* **41**(26), 5502–5509.

Frey, M.M. *and 6 others*. 2009. Contrasting atmospheric boundary layer chemistry of methylhydroperoxide (CH_3OOH) and hydrogen peroxide (H_2O_2) above polar snow. *Atmos. Chem. Phys.,* **9**(10), 3261–3276.

Gerland, S. *and 6 others*. 1999. Physical and optical properties of snow covering Arctic tundra on Svalbard. *Hydrol. Process.,* **13**(14/15), 2331–2343.

Grannas, A.M. *and 11 others*. 2002. A study of photochemical and physical processes affecting carbonyl compounds in the Arctic atmospheric boundary layer. *Atmos. Environ.,* **36**(15–16), 2733–2742.

Grannas, A.M., W.C. Hockaday, P.G. Hatcher, L.G. Thompson and E. Mosley-Thompson. 2006. New revelations on the nature of organic matter in ice cores. *J. Geophys. Res.,* **111**(D4), D04304. (10.1029/2005JD006251.)

Grannas, A.M. *and 34 others*. 2007. An overview of snow photochemistry: evidence, mechanisms and impacts. *Atmos. Chem. Phys.,* **7**(16), 4329–4373.

Grenfell, T.C. and G.A. Maykut. 1977. The optical properties of ice and snow in the Arctic Basin. *J. Glaciol.*, **10**(80), 445–463.

Guimbaud, C. *and 10 others*. 2002. Snowpack processing of acetaldehyde and acetone in the Arctic atmospheric boundary layer. *Atmos. Environ.,* **36**(15–16), 2743–2752.

Heaton, T.H.E., P. Wynn and A.M. Tye. 2004. Low $^{15}N/^{14}N$ ratios for nitrate in snow in the High Arctic (79°N). *Atmos. Environ.,* **38**(33), 5611–5621.

Honrath, R.E., S. Guo, M.C. Peterson, M.P. Dziobak, J.E. Dibb and M.A. Arsenault. 2000. Photochemical production of gas phase NO_x from ice crystal NO_3^-. *J. Geophys. Res.,* **105**(D19), 24,183–24,190.

Honrath, R.E. *and 6 others*. 2002. Vertical fluxes of NO_x, HONO, and HNO_3 above the snowpack at Summit, Greenland. *Atmos. Environ.,* **36**(15–16), 2629–2640.

Houdier, S. *and 9 others*. 2002. Acetaldehyde and acetone in the Arctic snowpack during the ALERT2000 campaign. Snowpack composition, incorporation processes and atmospheric impact. *Atmos. Environ.,* **36**(15–16), 2609–2618.

Hutterli, M.A., R. Röthlisberger and R.C. Bales. 1999. Atmosphere-to-snow-to-firn transfer studies of HCHO at Summit, Greenland. *Geophys. Res. Lett.*, **26**(12), 1691–1694.

Hutterli, M.A., J.R. McConnell, R.C. Bales and R.W. Stewart. 2003. Sensitivity of hydrogen peroxide (H_2O_2) and formaldehyde (HCHO) preservation in snow to changing environmental conditions: implications for ice core records. *J. Geophys. Res.,* **108**(D1), 4023. (10.1029/2002JD002528.)

Hutterli, M.A., J.R. McConnell, G. Chen, R.C. Bales, D.D. Davis and D.H. Lenschow. 2004. Formaldehyde and hydrogen peroxide in air, snow and interstitial air at South Pole. *Atmos. Environ.,* **38**(32), 5439–5450.

Jacobi, H.-W. and B. Hilker. 2007. A mechanism for the photochemical transformation of nitrate in snow. *J. Photochem. Photobiol. A,* **185**(2–3), 371–382.

Jacobi, H.-W., T. Annor and E. Quansah. 2006. Investigation of the photochemical decomposition of nitrate, hydrogen peroxide, and formaldehyde in artificial snow. *J. Photochem. Photobiol. A,* **179**(3), 330–338.

Jones, A.E., R. Weller, E.W. Wolff and H.W. Jacobi. 2000. Speciation and rate of photochemical NO and NO_2 production in Antarctic snow. *Geophys. Res. Lett.,* **27**(3), 345–348.

Jones, A.E. *and 6 others*. 2001. Measurements of NO_x emissions from the Antarctic snowpack. *Geophys. Res. Lett.,* **28**(8), 1499–1502.

King, D. and W.R. Simpson. 2001. Extinction of UV radiation in Arctic snow at Alert, Canada (82°N). *J. Geophys. Res.,* **106**(D12), 12,499–12,507.

Kleffmann, J. 2007. Daytime sources of nitrous acid (HONO) in the atmospheric boundary layer. *ChemPhysChem,* **8**(8), 1137–1144.

Lee-Taylor, J. and S. Madronich. 2002. Calculation of actinic fluxes with a coupled atmosphere–snow radiative transfer model. *J. Geophys. Res.,* **107**(D24), 4796. (10.1029/2002JD002084.)

https://doi.org/10.3189/002214310793146250 Published online by Cambridge University Press

Mabilia, R., V. Di Palo, C. Cassardo, C. Ciuchini, A. Pasini and M. Possanzini. 2007. Measurements of lower carbonyls and hydrocarbons at Ny-Ålesund, Svalbard. *Ann. Chim.,* **97**(10), 1027–1037.

Mack, J. and J.R. Bolton. 1999. Photochemistry of nitrite and nitrate in aqueous solution: a review. *J. Photochem. Photobiol. A,* **128**(1–3), 1–13.

McConnell, J.R., J.R. Winterle, R.C. Bales, A.M. Thompson and R.W. Stewart. 1997. Physically based inversion of surface snow concentrations of H_2O_2 to atmospheric concentrations at South Pole. *Geophys. Res. Lett.*, **24**(4), 441–444.

McConnell, J.R., R.C. Bales, R.W. Stewart, A.M. Thompson, M.R. Albert and R. Ramos. 1998. Physically based modeling of atmosphere-to-snow-to-firm transfer of H_2O_2 at south pole. *J. Geophys. Res.,* **103**(D9), 10,561–10,570.

McPeters, R.D. *and 13 others*. 1998. *Earth Probe Total Ozone Mapping Spectrometer (TOMS) data products user's guide*. Greenbelt, MD, NASA Goddard Space Flight Center. (NASA Tech. Publ. 1998-206895.)

Morin, S. *and 6 others*. 2008. Tracing the origin and fate of NO_x in the Arctic atmosphere using stable isotopes in nitrate. *Science,* **322**(5902), 730–732.

Nickus, U. 2003. Ion content of the snowpack on Franz Josef Land, Russia. *Arct. Antarct. Alp. Res.,* **35**(3), 399–408.

Oncley, S.P., M. Buhr, D.H. Lenschow, D. Davis and S.R. Semmer. 2004. Observations of summertime NO fluxes and boundary-layer height at the South Pole during ISCAT 2000 using scalar similarity. *Atmos. Environ.,* **38**(32), 5389–5398.

Opel, T. *and 10 others*. 2009. 115 year ice-core data from Akademii Nauk ice cap, Severnaya Zemlya: high-resolution record of Eurasian Arctic climate change *J. Glaciol.*, **55**(189), 21–31.

Phillips, G.J. and W.R. Simpson. 2005. Verification of snowpack radiation transfer models using actinometry. *J. Geophys. Res.,* **110**(D8), D08306. (10.1029/2004JD005552.)

Qian, Y., W.I. Gustafson, L.R. Leung and S.J. Ghan. 2009. Effects of soot-induced snow albedo change on snowpack and hydrological cycle in western United States based on weather research and forecasting chemistry and regional climate simulations. *J. Geophys. Res.,* **114**(D3), D03108. (10.1029/2008JD011039.)

Semb, A., R. Brækkan and E. Joranger. 1984. Major ions in Spitsbergen snow samples. *Geophys. Res. Lett.*, **11**(5), 445–448.

Shepson, P.B. *and 6 others*. 1996. Sources and sinks of carbonyl compounds in the arctic ocean boundary layer: polar ice floe experiment. *J. Geophys. Res.*, **101**(D15), 21,081–21,089.

Simpson, W.R., M.D. King, H.J. Beine, R.E. Honrath and X. Zhou. 2002. Radiation-transfer modeling of snow-pack photochemical processes during ALERT 2000. *Atmos. Environ.,* **36**(15–16), 2663–2670.

Stamnes, K., S.C. Tsay, W. Wiscombe and K. Jayaweera. 1988. Numerically stable algorithm for discrete-ordinate-method radiative transfer in multiple-scattering and emitting layered media. *Appl. Opt.*, **27**(12), 2502–2509.

Sturm, M., J. Holmgren and G.E. Liston 1995. A seasonal snow cover classification system for local to global applications. *J. Climate*, **8**(5), 1261–1283.

Sumner, A.L. and P.B. Shepson 1999. Snowpack production of formaldehyde and its effect on the Arctic troposphere. *Nature*, **398**(6724), 230–233.

Warren, S.G. 1982. Optical properties of snow. *Rev. Geophys.*, **20**(1), 67–89.

Warren, S.G. and R.E. Brandt. 2008. Optical constants of ice from the ultraviolet to the microwave: a revised compilation. *J. Geophys. Res.,* **113**(D14), D14220. (10.1029/2007JD009744.)

Wolff, E.W., J.S. Hall, R. Mulvaney, E.C. Pasteur, D. Wagenbach and M. Legrand. 2002. Modelling photochemical NO_x production and nitrate loss in the upper snowpack of Antarctica. *Geophys. Res. Lett.,* **29**(20), 1944. (10.1029/2002GL015823.)

Zhou, X. *and 6 others*. 2001. Snowpack photochemical production of HONO: a major source of OH in the Arctic boundary layer in springtime. *Geophys. Res. Lett.,* **28**(21), 4087–4090.

MS received 20 October 2009 and accepted in revised form 5 June 2010